CrystEngComm

COMMUNICATION

View Article Online
View Journal | View Issue

Cite this: *CrystEngComm*, 2018, **20**, 5935

Received 24th April 2018,
Accepted 14th June 2018

DOI: 10.1039/c8ce00652k

rsc.li/crystengcomm

A H-shaped heterometallic Sn_4Au_4 system with guest-tuneable multicolour and selective luminescence sensing properties†

Csaba Jobbágy,[a] Péter Baranyai,‡[a] Ágnes Gömöry[b] and Andrea Deák *[a]

A H-shaped heterometallic Sn_4Au_4 system that displays tuneable guest-dependent optical and photoluminescent properties has been synthesized. It shows selective dye sorption, while its stimuli-responsive methylred-rich solid is sensitive towards pH variations. This non-emissive Sn_4Au_4 system exhibits multicolour luminescence in the presence of aniline derivatives.

Coordination-driven supramolecular self-assembly has been proved to be exceptionally efficient in the development of heterometallic supramolecules with intriguing physical and chemical properties.[1–5] Multifunctional ligands bearing various donor atoms offer opportunities to combine a variety of different metal centres and therefore to produce an impressive diversity of heterometallic supramolecular assemblies, which comprise macrocycles, cages, clusters, coordination polymers, networks and metal–organic frameworks.[5–11] The design and synthesis of heterometallic supramolecules incorporating main group and transition elements is, however, still challenging due to the differences in coordination and electronic properties of metal centers.[12–14] As part of our studies, we reported the coordination-driven assembly of main group metal units (Me_3Sn^+ and Me_2Sn^{2+}) with gold(I)-based bridging metalloligand ($[Au(CN)_2]^-$) leading to coordination polymeric arrays with striking stimuli-responsive mechanochromic luminescence.[4]

Despite the considerable progress which has been achieved in the construction of porous solids based on metal–organic frameworks (MOFs), porous organic frameworks (POFs) and discrete organic molecules,[15–19] the exploration of discrete heterometallic complexes for the development of materials with guest-tuneable photophysical properties remains in its infancy.[11] The vast majority of reports on this topic, however, deals with the guest-dependent photophysical properties of MOFs and POFs, which have definable pore size and shapes.[15–17] MOFs have been extensively utilized as hosts to encapsulate chromophore guests such as dyes, however only a limited number of MOF@dye composite systems have been exploited for vapour-based chemical sensing of various volatile organic compounds (VOC's).[5]

Design of crystal structures from well-defined molecular building blocks is still a major challenge due to the large complexity of possible solid-state structures. H-shaped molecules offer a simplification in crystal engineering strategies by reducing the number of possible packing patterns mainly into either ladder or brick-wall arrangements (Scheme 1).[20]

As shown in Scheme 1, these molecular arrangements generate void spaces, which are filled with appropriate guest (usually solvent) molecules. These cavities often collapse when guest molecules are removed, although they could be restored upon guest binding. This is especially important for obtaining guest-dependent optical and stimuli-responsive properties. Although there are numerous examples on the crystal engineering of organic H-shaped molecules,[20–22] to

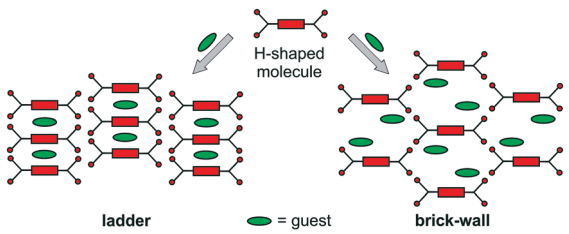

Scheme 1 Typical ladder and brick-wall crystal packing patterns of the H-shaped molecules providing void spaces filled with guest molecules.

[a] *MTA TTK SZKI, "Lendület" Supramolecular Chemistry Research Group, Hungarian Academy of Sciences, Magyar Tudósok körútja 2, 1117 Budapest, Hungary. E-mail: deak.andrea@ttk.mta.hu*

[b] *MTA TTK SZKI, MS Proteomics Research Group, Hungarian Academy of Sciences, Magyar Tudósok körútja 2, 1117 Budapest, Hungary*

† Electronic supplementary information (ESI) available: Experimental details and additional figures. CCDC 1563281 and 1563282. For ESI and crystallographic data in CIF or other electronic format see DOI: 10.1039/c8ce00652k

‡ Present address: Department of Applied and Nonlinear Optics, Wigner Research Centre for Physics of the Hungarian Academy of Sciences, Institute for Solid State Physics and Optics, 1121 Budapest, Konkoly-Thege Miklós út 29-33, Hungary.

our knowledge only a pentiptycene-derived structures have been used to sense diverse volatile organic compounds.[23–27] For example, the green-fluorescent H-shaped pentiptycene scaffold creates pores accessible to guest molecules in the solid state and shows exceptional guest-dependent luminescent properties owing to ground-state host–guest interactions and excited-state exciplex formation.[23] This prompted us to investigate if it might be possible to modulate the photophysical properties of H-shaped metallosupramolecular systems by guest molecules. To our knowledge, there are no studies focusing on the photophysical properties of discrete heterometallic H-shaped host, though the understanding of guest-responsive optical and luminescent properties of such systems is important for the design of novel functional materials.

To create a H-shaped heterometallic system, it is essential to develop a metalloligand having four donor sites and more importantly to favourable preorganise them. H-shaped structures are typical for $\{[Me_2Sn(RCOO)]_2O\}_2$ organostannoxanes,[28] thus, we expected that a bifunctional ligand, namely 4-diphenylphosphinobenzoic acid (Hdppba) functionalized with O- and P-donor sets might create an organostannoxanic $\{[Me_2Sn(dppba)]_2O\}_2$ complex (**1**, Scheme 2). This tetranuclear complex containing four Sn(IV) and four Ph_2P sites would be an ideal H-shaped metalloligand that can further coordinate Au(I) centres with its arms. The as-resulting bulky H-shaped heterometallic $\{[Me_2Sn(dppba)(AuCl)]_2O\}_2$ (**2**, Scheme 2) system with π-electron rich parts can be anticipated to show intriguing guest-responsive properties.

The phosphine-functionalized metalloligand **1** was synthesized by the reaction of Me_2SnO with Hdppba following the general method (Scheme S1, route i, for details see the ESI†). The H-shaped metalloligand **1** features four dangling phosphine-donor groups suitable for binding to second metal species through metal–ligand bonds, in the next step, when mixed at the correct stoichiometric ratio. Accordingly, the addition of stoichiometric amounts of $(Me_2S)AuCl$ to **1** (Scheme S1, route ii, ESI†) results in the formation of a octametallic Sn_4Au_4 molecular clip (**2**). The singlet at 32.9 ppm observed in the ^{31}P NMR spectrum of **2** is downfield shifted compared to **1** (Fig. S2 and S6, ESI†), which indicates the coordination of phosphorous centres of the metalloligand to Au(I). The presence of two chemically non-equivalent Sn(IV) sites is demonstrated by two peaks at −174.8 and −190.6 ppm in the ^{119}Sn NMR spectrum (Fig. S7†) and confirms that the tetraorganodistannoxanic core of the metalloligand **1** (Fig. S3†) remains practically unaltered after P–Au bond formation.

The single-crystal XRD analysis of colourless crystals of **1**·$1.23CH_2Cl_2$ reveals that the complex has a H-shaped structure (Fig. 1) typical for $\{[Me_2Sn(RCOO)]_2O\}_2$ organostannoxanes[28] with a core made up by a planar Sn_2O_2 ring and two additional Sn centres supported by the bridging and chelate-bridging carboxylate groups of the ligand (Table S2, ESI†). Complex **1** lies on an inversion centre, which is at the centre of the Sn_2O_2 ring.

The X-ray structure of colourless **2**·$3.88CH_2Cl_2$ shows the formation of the anticipated octametallic Sn_4Au_4 assembly, wherein the closely linear coordination of the dangling phosphine-donor groups of **1** to AuCl created a H-shaped heterometallic structure (Fig. 2). The central core of **2** consists of planar Sn_2O_2 ring and two additional Sn centres supported by two bridging and two monoatomic bridging carboxylate groups of the dppba ligand. This heterometallic derivative of **1** similarly resides on an inversion centre located at the centre of the Sn_2O_2 ring. The bulky H-shaped molecular clip comprises the Au(I) centres at a distance of 10.736(2) Å [Au1···Au2*; wherein Au2* is at $1 - x$, $2 - y$, $-z$] and 19.774(2) Å [Au1···Au2], respectively.

As shown in Fig. 3a, the crystal structure shows that the metalloligand **1** molecules are arranged in ladder pattern and the solvent molecules are encapsulated in discrete voids (Fig. S9, ESI†). The potential void volume accessible for guest molecules upon CH_2Cl_2 removal is as low as 208.1 $Å^3$ (9.9% of the unit cell volume of 2102.2 $Å^3$) calculated by the PLATON program.[29] The crystal structure of **2** consists of H-shaped Sn_4Au_4 molecular clips arranged in brick-wall pattern (Fig. 3b) *via* C–H···Cl–Au contacts (Fig. S11, ESI†). The CH_2Cl_2 molecules are hosted in the channels having large dumbbell-shaped cavities (Fig. 3b). The high guest-accessible void volume is 1588.5 $Å^3$ (28.5% of the unit cell volume of 5571.5 $Å^3$) calculated by PLATON,[29] is available for guest

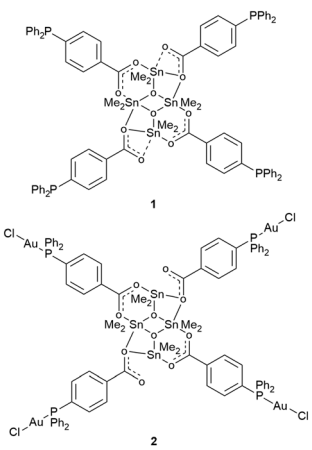

Scheme 2 H-shaped metalloligand **1** and its gold(I) decorated complex **2**.

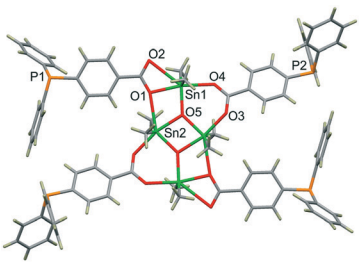

Fig. 1 Molecular structure of H-shaped metalloligand **1**. Colour scheme: tin, green; phosphorous, orange; carbon, grey; oxygen, red; hydrogen, dark brown.

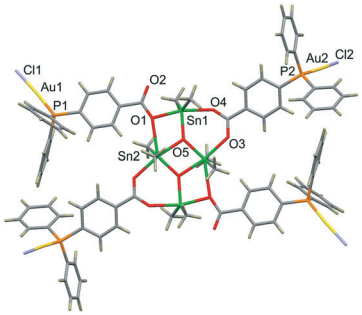

Fig. 2 Molecular structure of H-shaped heterometallic **2**. Colour scheme: tin, green; gold, yellow; phosphorous, orange; carbon, grey; oxygen, red; chlorine, purple; hydrogen, dark brown.

inclusion upon exchange with solvent molecules (Fig. S10, ESI†).

Metalloligand **1** is not luminescent in solution at 298 K, however in the solid state it exhibits a bright green emission centred at 502 nm (Fig. S12†) with luminescence quantum yield (φ_{em}) of 0.14 and lifetime (τ_{em}) of 4.2 ns, which is comparable to that of the dppba ligand (Table S3, ESI†). This suggests that the emission is fluorescence caused by the rigidification mediated by restriction of intramolecular motion and there is no participation of the metal ions in the excited states which was confirmed by the quantum chemical calculations (for details see the ESI†). The emission intensity from metalloligand **1** to its gold(I)-coordinated complex **2** decreases significantly, and the octametallic Sn_4Au_4 system is practically non-luminescent in the solid state (Fig. S12 and Table S3, ESI†). The strong luminescence quenching upon Au(I) coordination reflects the importance of the lone pair of phosphorous atoms in the radiative transition of **1** (Fig. S18 and S20†). Moreover, it is very intriguing that the binding of diverse types of metal ions to different donor sites of dppba ligand allows us to regulate the luminescence properties selectively.

Next, we anticipated that the large openings (the void diameter calculated by Poreblazer[30] ranges from 12.3 to 14.4 Å) of **2** would allow the access, passage, exchange and inclusion of larger chromophoric guest species such as organic dyes. Typically, the freshly prepared colourless crystals of **2** were immersed into aqueous solution of various dyes including neutral methylred (MR), cationic methylene blue (MB) and anionic methylene orange (MO). The colourless crystals of **2** became deep red (Fig. 4a) as well as blue (Fig. 4b) indicating the formation of dye-rich solid **2**, while the anionic MO dye molecules were not diffused into crystals of **2**.

Because the dyed crystals typically include dye molecules at the parts per thousand to parts per million level, X-ray diffraction is practically useless for determining the structure of such dye inclusion compounds.[31] As in the case of other dyed crystals, the inclusion and uniformity of distribution of dye guests in the crystal is difficult to determine directly, thus the incorporation of dyes was verified visually.[32–34] As shown in Fig. 4, the shape and integrity of crystals of **2** remained intact after standing in aqueous dye solutions for 7 days, while a colour change into either deep red (MR) or blue (MB) provided the optical evidence of dye inclusion. The dye inclusion uniformity was also verified by optical microscopy (Fig. S21, ESI†). Moreover, mass spectrometric measurements indicate that 1 mole of dye-rich crystals of **2** contains 2–3 × 10^{-3} moles of dye (either MR or MB) molecules (Fig. S24 and S25, ESI†).

The selective adsorption of MR and MB over the MO in water may be caused by the differences in the molecular size, as MR and MB have smaller molecular diameter (13.2 and 13.4 Å, respectively) than that of MO (14.5 Å).[35,36] Other molecular characteristics of dyes (shape, charge, hydrogen and π···π bonding ability, *etc.*) might also affect the dye adsorption selectivity.[35,36] In contrast to intriguing dye absorption ability shown by **2**, the crystals of **1** cannot capture these dye molecules, as no significant guest-accessible void volumes are present in the structure (Fig. S22, ESI†).

Smart solid-state materials, which sensitively respond to external stimuli with dramatic changes in their solid-state optical properties such as colour[15,16] and/or luminescence[37–40] are of particular interest as they can be used to monitor environmental changes. Stoddart and co-workers have shown that MOF's incorporating pH-sensitive dyes display colorimetric changes in the presence of acid/base vapours.[15,16] For example, a MOF with incorporated anionic MR^- changes its colour from yellow to red in response to gaseous CO_2.[15]

Inspired by these results, the MR-rich solid **2** was tested to act as a colorimetric switch, whereby the pH-sensitive dye molecules can sensitively respond to acid and base vapours. The orange-yellow colour of the azobenzene-based pH-indicator MR is generally associated with the neutral MR^0, the red colour with zwitterionic $MR^{\pm}$ and protonated MRH^+ forms, while the yellow colour with the deprotonated MR^- species (Fig. S26, ESI†).[41] We might then reasonably assume that the

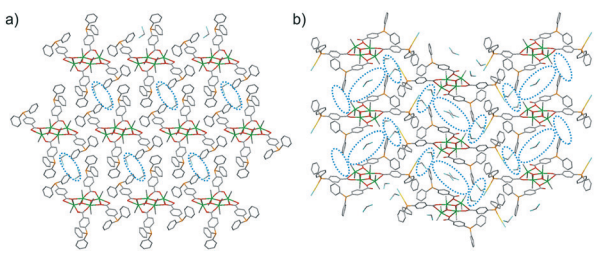

Fig. 3 a) Ladder-type packing of **1** and b) brick wall molecular arrangement of **2** (view along the crystallographic *a*-axis). The CH_2Cl_2 solvent molecules are marked with dotted ice-blue line. The hydrogen atoms are omitted for clarity.

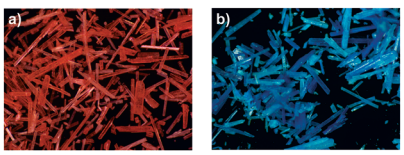

Fig. 4 Colorimetric response of **2** to a) MR and b) MB dye molecules, respectively.

red-coloured solid 2 is enriched with zwitterionic forms of MR. We observed a colour change from red to yellow when the MR-rich solid 2 was exposed to gaseous ammonia, which suggests that the NH_3 abstracted protons from the zwitterions resulting in a yellow-coloured anionic MR-rich solid 2 (Fig. 5a). The colour change was reversible, and following exposure to HCl, the MR^- anion undergoes protonation to regenerate the red-coloured zwitterionic or protonated MR-rich solid 2 (Fig. 5b). As in the case of other acidochromic systems, each deprotonation/protonation cycle triggered by NH_3/HCl vapour also gives rise to the formation of ammonium chloride in the system.[42] It should be noted that humid CO_2 (from sublimed dry ice, Fig. S28 ESI†) can also regenerate the red-coloured MR-functionalized solid 2. The NH_3/HCl vapour triggered reversible colorimetric response occurred quickly, and after 3 min, no further significant colour change was observed. This cycle was repeated more than 4 times without noticeable decrease in the sensitivity and colour intensity. It is worth noting that, in contrast to this acidochromic MR-rich solid 2 the pristine MR dye cannot be practically actuated by acid/base vapours in the solid state (Fig. S29 ESI†).

Inspired by these results, we finally explored the sensing capability of 2 for monitoring the presence of VOC's. The guest-responsive luminescence properties of 2 were investigated with a series of aniline derivatives, including aniline (AN) and its various electron-rich derivatives such as *N*,*N*-dimethylaniline (DMA), *N*,*N*-diethylaniline (DEA) and 4,*N*,*N*-trimethylaniline (TMA) as well as electron-deficient analogues such as 3-fluoroaniline (FA) and 3,5-bis(trifluoromethyl)aniline (BTFMA). Thin-layered powdered sample of 2 was exposed to the vapours of these various aniline derivatives, and as shown in Fig. 6a, the luminescence of 2 rapidly turns on after exposure to AN, FA, TMA, DMA and DEA vapours (see ESI†). No significant luminescence response was observed for BTFMA vapours. The emission colour of aniline-rich solid 2 (Fig. 6b) depended on the aniline and was bluish green with FA (508 nm), dark green with AN (534 nm) and greenish yellow with DMA (558 nm), DEA (561 nm) and TMA (552 nm), respectively. The spectral shifts appear to correlate most closely with the electron-donating ability of these aniline vapours, as derivatives with electron-donating methyl group(s) induced greater red-shifts than electron-withdrawing fluorine substituted anilines. Accordingly, the TMA and DMA triggers the most obvious luminescence response and an intense greenish yellow emission appeared, along with a 471- and 591-fold luminescence enhancement, respectively. It is important to note that the luminescence of 2 remains unchanged upon exposure to aliphatic amines (triethylamine and diethylamine) and aromatic hydrocarbons (toluene and xylene) vapours. This suggests the synergetic effects of the amine group and π-electron rich system of the aniline derivatives on the luminescence turn on of 2. Thus, the sensing ability could be mainly attributed to favourable interactions between H-shaped heterometallic host having π-electron rich parts and aromatic amine guests.

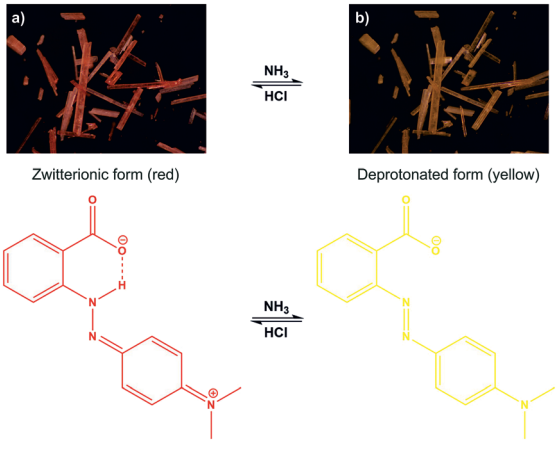

Fig. 5 Colorimetric response the MR-rich solid 2 during the acid/base sensing process. a) Red-coloured zwitterionic MR-rich crystals of 2 changed into yellow-coloured anionic MR-rich solid when exposed to NH_3 vapours and b) back from yellow to red when exposed to HCl vapours.

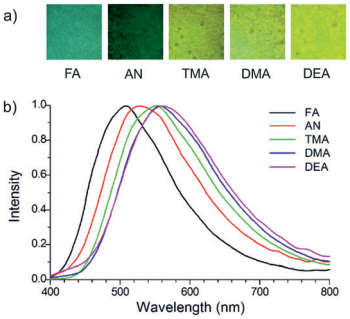

Fig. 6 Luminescence turn on response of crystalline 2 to aniline derivatives: a) optical microscope images of 2 upon exposure to various aniline vapours under 365 nm UV lamp illumination and b) their normalized solid-state emission spectra (λ_{exc} = 365 nm).

In summary, we constructed the first heterometallic H-shaped Sn_4Au_4 molecular clip that displays tuneable guest-dependent optical and photoluminescent behaviour. The molecular packing of this bulky H-shaped molecular clip 2 creates guest-accessible voids in the solid state, which would enable the realization of guest-tuneable photophysical behaviour previously unseen for discrete heterometallic systems. Its stimuli-responsive MR-rich solid 2 shows sensitivity towards variations in the pH value and indicates these alterations in environmental conditions by intense colorimetric changes from red to yellow. Moreover, this heterometallic solid 2 can be used as a luminescent sensory system to reliably distinguish between different aniline derivatives. This new strategy toward guest-responsive heterometallic materials shows that a single chromophoric host is sufficient for multicolour optical and luminescence tuning by guest molecules. The present study illustrates that the synthesis of bulky H-shaped heterometallic complexes would open up a new strategy to construct various stimuli-sensitive materials, serving as potential candidates in the development of a new class of functional supramolecular materials with intriguing sensing applications.

This work was supported by the Hungarian Academy of Sciences through the Lendület Programme (LP2012-21/2012).

Conflicts of interest

There are no conflicts to declare.

Notes and references

1 M. L. Saha, X. Yan and P. J. Stang, *Acc. Chem. Res.*, 2016, **49**, 2527–2539.
2 X. Yan, T. R. Cook, P. Wang, F. Huang and P. J. Stang, *Nat. Chem.*, 2015, **7**, 342–348.
3 X. Yan, H. Wang, C. E. Hauke, T. R. Cook, M. Wang, M. L. Saha, Z. Zhou, M. Zhang, X. Li, F. Huang and P. J. Stang, *J. Am. Chem. Soc.*, 2015, **137**, 15276–15286.
4 C. Lescop, *Acc. Chem. Res.*, 2017, **50**, 885–894.
5 L. Schneider, V. Sivchik, K. Y. Chung, Y. T. Chen, A. J. Karttunen, P. T. Chou and I. O. Koshevoy, *Inorg. Chem.*, 2017, **56**, 4460–4468.
6 F. A. Cotton, J. Y. Jin, Z. Li, C. Y. Liu and C. A. Murillo, *Dalton Trans.*, 2007, 2328–2335.
7 J. Wu, L. Zhao, L. Zhang, X. L. Li, M. Guo, A. K. Powell and J. Tang, *Angew. Chem., Int. Ed.*, 2016, **55**, 15574–15578.
8 H. Sepehrpour, M. L. Saha and P. J. Stang, *J. Am. Chem. Soc.*, 2017, **139**, 2553–2556.
9 S. A. Baudron and M. W. Hosseini, *Chem. Commun.*, 2016, **52**, 13000–13003.
10 V. Vajpayee, H. Kim, A. Mishra, P. S. Mukherjee, P. J. Stang, M. H. Lee, H. K. Kim and K. W. Chi, *Dalton Trans.*, 2011, **40**, 3112–3115.
11 J. Ferrando-Soria, H. Khajavi, P. Serra-Crespo, J. Gascon, F. Kapteijn, M. Julve, F. Lloret, J. Pasan, C. Ruiz-Perez, Y. Journaux and E. Pardo, *Adv. Mater.*, 2012, **24**, 5625–5629.
12 S. Hazra, R. Meyrelles, A. J. Charmier, P. Rijo, M. F. Guedes da Silva and A. J. Pombeiro, *Dalton Trans.*, 2016, **45**, 17929–17938.
13 A. Deák, T. Tunyogi and G. Pálinkas, *J. Am. Chem. Soc.*, 2009, **131**, 2815–2817.
14 C. Jobbágy, T. Tunyogi, G. Pálinkas and A. Deák, *Inorg. Chem.*, 2011, **50**, 7301–7308.
15 J. J. Gassensmith, H. Furukawa, R. A. Smaldone, R. S. Forgan, Y. Y. Botros, O. M. Yaghi and J. F. Stoddart, *J. Am. Chem. Soc.*, 2011, **133**, 15312–15315.
16 S. Han, Y. Wei, C. Valente, R. S. Forgan, J. J. Gassensmith, R. A. Smaldone, H. Nakanishi, A. Coskun, J. F. Stoddart and B. A. Grzybowski, *Angew. Chem., Int. Ed.*, 2011, **50**, 276–279.
17 J. Dong, A. K. Tummanapelli, X. Li, S. Ying, H. Hirao and D. Zhao, *Chem. Mater.*, 2016, **28**, 7889–7897.
18 M. Yamashina, M. M. Sartin, Y. Sei, M. Akita, S. Takeuchi, T. Tahara and M. Yoshizawa, *J. Am. Chem. Soc.*, 2015, **137**, 9266–9269.
19 H. K. Chae, D. Y. Siberio-Perez, J. Kim, Y. Go, M. Eddaoudi, A. J. Matzger, M. O'Keeffe and O. M. Yaghi, *Nature*, 2004, **427**, 523–527.
20 T. Tanaka, T. Tasaki and Y. Aoyama, *J. Am. Chem. Soc.*, 2002, **124**, 12453–12462.
21 K. Endo, T. Sawaki, M. Koyanagi, K. Kobayashi, H. Masuda and Y. Aoyama, *J. Am. Chem. Soc.*, 1995, **117**, 8341–8352.
22 Y. Aoyama, K. Endo, T. Anzai, Y. Yamaguchi, T. Sawaki, K. Kobayashi, N. Kanehisa, H. Hashimoto, Y. Kai and H. Masuda, *J. Am. Chem. Soc.*, 1996, **118**, 5562–5571.
23 Y. Matsunaga and J.-S. Yang, *Angew. Chem., Int. Ed.*, 2015, **54**, 7985–7989.
24 J.-S. Yang, J. L. Yan, C. K. Lin, C. Y. Chen, Z. Y. Xie and C. H. Chen, *Angew. Chem., Int. Ed.*, 2009, **48**, 9936–9939.
25 J.-S. Yang, J.-L. Yan, C.-Y. Hwang, S.-Y. Chiou, K.-L. Liau, H.-H. Gavin Tsai, G.-H. Lee and S.-M. Peng, *J. Am. Chem. Soc.*, 2006, **128**, 14109–14119.
26 J.-S. Yang and T. M. Swager, *J. Am. Chem. Soc.*, 1998, **120**, 5321–5322.
27 J.-S. Yang and T. M. Swager, *J. Am. Chem. Soc.*, 1998, **120**, 11864–11873.
28 A. Deák and G. Tárkányi, in *Advances in Organometallic Chemistry Research*, ed. K. Yamamoto, Nova Science Publishers, Inc., New York, 2007, ch. 8, pp. 201–225.
29 A. L. Spek, *Acta Crystallogr., Sect. D: Biol. Crystallogr.*, 2009, **65**, 148–155.
30 L. Sarkisov and A. Harrison, *Mol. Simul.*, 2011, **37**, 1248–1257.
31 M. D. Hollingsworth, *Science*, 2002, **295**, 2410–2413.
32 B. Kahr and A. G. Shtukenberg, *CrystEngComm*, 2016, **18**, 8988–8998.
33 H. K. Chae, D. Y. Siberio-Pérez, J. Kim, Y. Go, M. Eddaoudi, A. J. Matzger, M. O'Keeffe and O. M. Yaghi, *Nature*, 2004, **427**, 523–527.
34 B. Kahr and R. W. Gurney, *Chem. Rev.*, 2001, **101**, 893–952.
35 Y. L. Li, Y. Zhao, P. Wang, Y. S. Kang, Q. Liu, X. D. Zhang and W. Y. Sun, *Inorg. Chem.*, 2016, **55**, 11821–11830.
36 W. Xie, W. W. He, S. L. Li, K. Z. Shao, Z. M. Su and Y. Q. Lan, *Chem. – Eur. J.*, 2016, **22**, 17298–17304.
37 C. Jobbágy and A. Deák, *Eur. J. Inorg. Chem.*, 2014, 4434–4449.
38 C. Jobbágy, M. Molnár, P. Baranyai, A. Hamza, G. Pálinkás and A. Deák, *CrystEngComm*, 2014, **16**, 3192–3202.
39 C. Jobbágy, P. Baranyai, G. Marsi, B. Rácz, L. Li, P. Naumov and A. Deák, *J. Mater. Chem. C*, 2016, **4**, 10253–10264.
40 A. Deák, C. Jobbágy, G. Marsi, M. Molnár, Z. Szakács and P. Baranyai, *Chem. – Eur. J.*, 2015, **21**, 11495–11508.
41 J. B. Benedict, D. E. Cohen, S. Lovell, A. L. Rohl and B. Kahr, *J. Am. Chem. Soc.*, 2006, **128**, 5548–5559.
42 P. K. Kundu, G. L. Olsen, V. Kiss and R. Klajn, *Nat. Commun.*, 2014, **5**, 3588.